Second Quarterly Technical Progress Report on Development and Testing of Electrolyte Matrix Combinations for Mercury-Potassium Fuel Cell (13 March — 12 June 1963)

Engineering Department Report No. 3455

NASA Contract NASw-476

This work is sponsored by the Space Power Technology Program of the NASA Headquarters. It is technically directed by Lewis Research Center, NASA, Cleveland, Ohio.

Allison Division

General Motors Corporation

Indianapolis, Indiana

Second Quarterly Technical Progress Report on Development and Testing of Electrolyte Matrix Combinations for Mercury-Potassium Fuel Cell (13 March — 12 June 1963)

Engineering Department Report No. 3455

10 July 1963

V. L. Decker
Project Manager
Research Activity

T. F. Nagey
Director of Research

TABLE OF CONTENTS

Section	Title	Page
I.	Introduction	1
II.	Second Quarter Progress	2
	Small LMC Operation	2
	Quality Control Studies	13
	Fabrication and Property Determination of Composites	23
	Coarse Grain Composite Work	23
	Fine Grain Composite Work	31
	Conductivity	31
	Mechanical Strength	34

LIST OF ILLUSTRATIONS

Figure	Title	Page
1.	Test Equipment for First Small Unit	3
2.	Posttest Analysis of Small Cell	3
3.	Silicon O-Ring Seal Test Teardown	5
4.	Small Cell Test Setup	7
5.	Small Cell Assembly	8
6.	Cell After Matrix Removal	11
7.	Section of Matrix from the Seal Region	12
8.	Second Cell Opened with Matrix in Place	14
9.	Matrix Removal from Second Small Cell	15
10.	Sections of Matrix from Second Cell Seal Region	16
11.	Test Rig for Compatibility Studies	17
12.	Electrolyte Matrix after Test Number 6—Note Cracks	19
13.	Broken Edges of Sixth Test Matrix—About 10% Bonded Through Cracked Area	20
14.	Micrographs of Broken Section of Seventh Test Composite Matrix	22
15.	Ball Penetration Strength Test Results	28
16.	Conductivity of Fine Grain Unconsolidated Electrolyte Matrices	35

LIST OF TABLES

Table	Title	Page
I.	Data on Composite Electrolyte Matrix Cell 1	9
II.	Ball Penetration Test Results—Coarse Grain Composites	24
III.	Flowability Test Results—Coarse Grain Composites	26
IV.	Ball Penetration Test Data—34/66 Coarse Grain Composite	29
V.	Flowability Test Data—34/66 Coarse Grain Composite	31
VI.	Conductivity Specimen Identification	32
VII.	Conductivity Specimen Data	33
VIII.	Ball Penetration Test Results—Fine Grain Composites	36
IX.	Flowability Test Data—Fine Grain Composites	37

I. INTRODUCTION

This is the second quarterly technical progress report on development and testing of electrolyte matrix combinations for mercury-potassium fuel cell for the period 13 March—12 June 1963. This work is being conducted under NASA Contract NASw-476.

A coarse grain composite, tested in a potassium-mercury cell has shown that the self-sealing matrix principle is sound. The performance parameters, γt_e, are near 3 ohm-cm^2, for a thickness, t_e, of 0.32 cm. However, it is not likely that an improvement factor of six—to meet system requirements—can be reached through a change in the thickness of the coarse grain composite.

Therefore, emphasis will be placed on the development of the fine grain composites. Conductivity data have shown that an improvement factor of two to three may be attained in the fine grain composite. A trade-off between resistivity and thickness in the use of matrix supporting members, screens, or perforated plates, appears to be the best approach to the attainment of this goal.

II. SECOND QUARTER PROGRESS

Significant progress has been made in the following areas: (1) operation of the small LMC; (2) fabrication of both coarse and fine grain MgO composites; and (3) development of improved quality control techniques for selection of composite.

SMALL LMC OPERATION

A description of the small cell studies was made in the first quarterly progress report, Allison EDR 3277. This description is repeated here for completeness. The test equipment design sketch is shown in Figure 1. Figure 2 shows the first small cell after test was completed.

This cell was designed to expose half of the 2-in. diameter disk to the liquid metal. This gives an active cell area of 0.785 in.^{2} (5.07 cm^2) and a seal area of 2.255 in.^{2}. It was intended that the liquid metal cavity wall angle would be adjusted by machining to obtain other ratios of active cell area to seal area. Modification was not made during this reporting period. Early work (prior to contract) with a 0.5-in. thick composite specimen and 5 psi differential pressure showed that this material is not permeable to argon gas. The seal region used for the test was that of the concentric serrations and was adopted for this small cell design. While no seal difficulties were anticipated at the time the work statement was set, the program depends on small cell seal design, with some optimization to be defined between seal area, leak-path length, serration depth, and serration width.

Work during the first quarter showed that some compositions highly saturated with electrolyte have high flowability characteristics (reference First Quarterly Technical Progress Report, Table V). This characteristic of the paste electrolyte led to the design of a mechanical stop to limit the deformation of the specimen in the cell. The stop is formed by a machined ceramic ring mounted within grooves on the two halves of the cell. Thus, sealing is accomplished by the electrolyte on the surface which wets the metal. Whether this is a chemical or surface tension type seal will be determined by testing during the next report period.

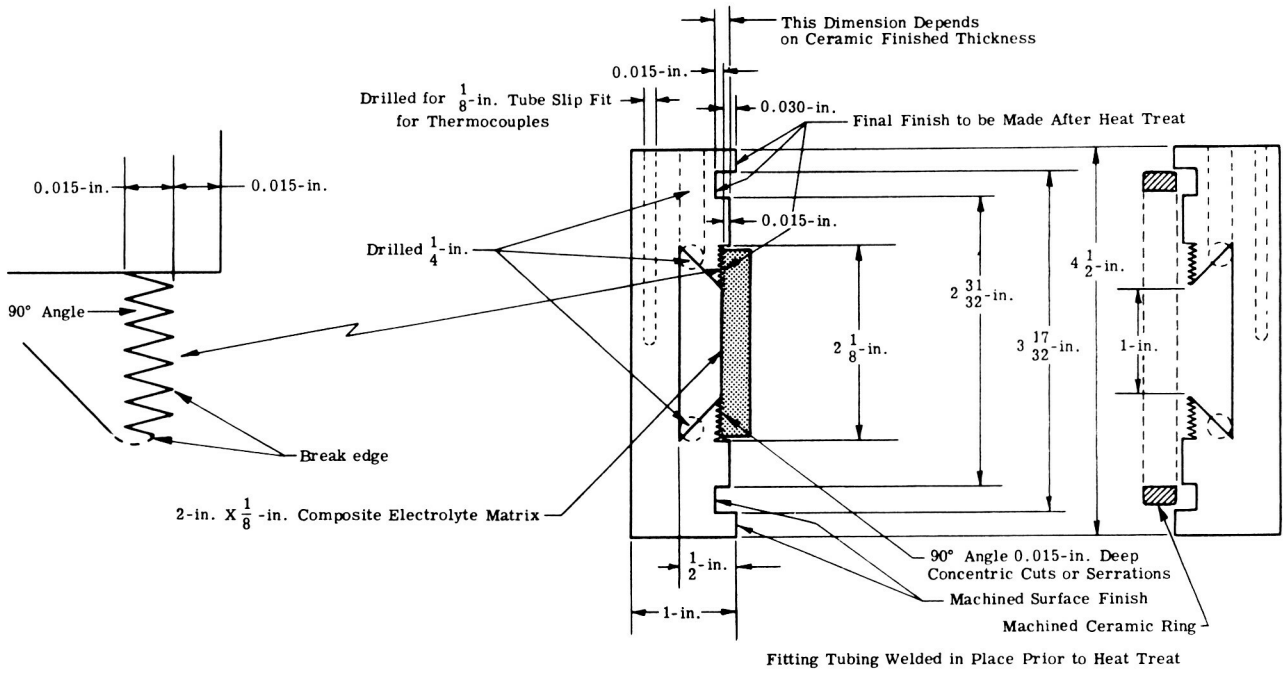

Figure 1. Test Equipment for First Small Unit

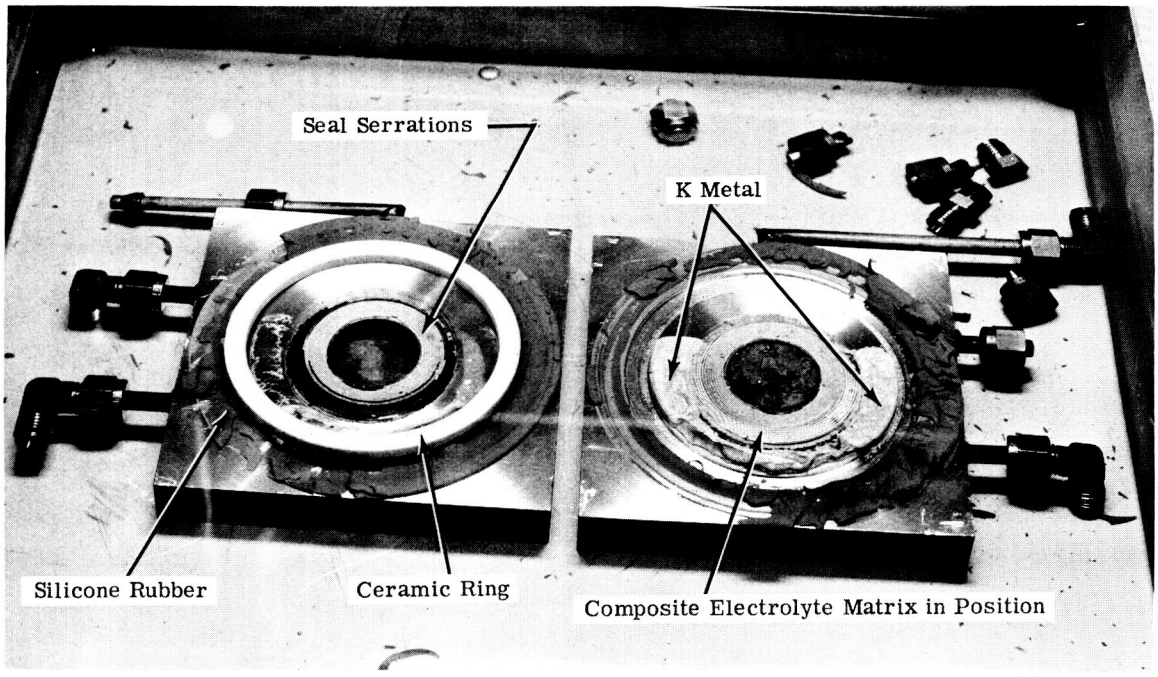

Figure 2. Posttest Analysis of Small Cell

The internal cell must be kept isolated from ambient conditions. Edges of the composite specimen will pick up CO_2 and water vapor which could weaken the seal. Therefore, a high temperature silicone rubber is incorporated at the outside of the mating surfaces. This material was tested in a number of cell configurations prior to the present program.

A special test was performed to determine that the silicone rubber could be used in the form of a small O-ring in the assembly of a composite matrix cell. A 35-hr test was performed while manipulating the flange tightening sequences in a manner simulating actual cell operation. Figure 3 shows the results of this test. To separate the plates after cool down, it was necessary to pry them open. Although the rubber was torn apart, it remained in contact with the metal at all points. This indicates extreme bonding characteristics which will ensure a good seal.

Other observed properties of the silicone rubber are:

1. An excess of electrolyte will break the rubber down into a liquid.

2. Limited contact with electrolyte causes a brittle substance which remains functional as a seal.

3. Compatibility with potassium and mercury is excellent.

4. Some reaction is evident with electrolyte-saturated potassium. However, limited contact as occurs with the edge of a seal does not cause seal failure, but only forms a limited amount of brittle material.

The silicone rubber in the design is shown outside the ceramic ring in Figures 1 and 2. However, its use inside this ring is possible if it is required to seal the liquid metals that bypass the intended composite seal.

Provisions can be made to incorporate a supporting member (screen or perforated plate) to oppose differential pressure across the matrix. The

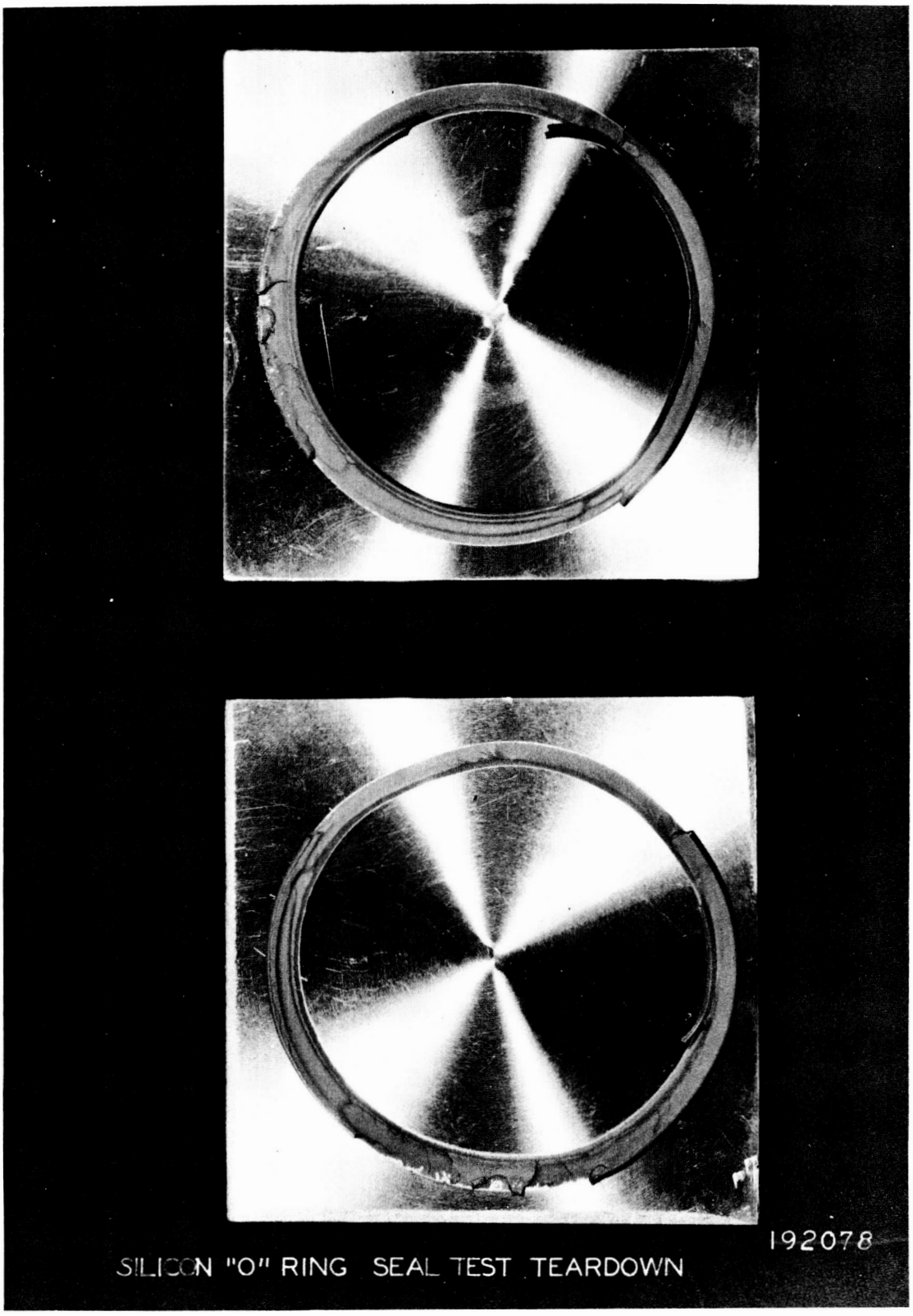

Figure 3. Silicon "O" Ring Seal Test Teardown

differential pressure in this case would be caused by a difference in the head-density products of the two opposing liquid metals. Therefore, this screen would be placed on the potassium side of the matrix.

The small cell test setup is shown in Figure 4. The cell assembly and all auxiliary components are made an integral part of a small furnace. The procedure for loading the electrolyte matrix is as follows.

1. The cell halves are placed in an inert glove box along with the matrix, ceramic ring, and silicone rubber seal.

2. The unit is assembled in the horizontal position with the oversized rubber taking the top-half load.

3. The assembly is removed from the dry box, with all lines sealed, and placed in the furnace. The furnace is positioned on the left side during this time.

4. After the clamp is applied and all line connections are made, the furnace is brought up to temperature while the cell is slowly closed. This ensures that the matrix is not damaged prior to becoming a paste.

5. The entire test rig is rotated to the position as shown in Figures 4 and 5.

The procedure for loading the liquid metal is as follows.

1. Potassium is introduced to the K-feed reservoir and later let down to the cell by the valve shown. The level is noted in the K-level indicator at right.

2. Mercury is loaded to the Hg feed reservoir and then let down to the Hg preheater at a rate sufficient to bring material up to near cell temperature.

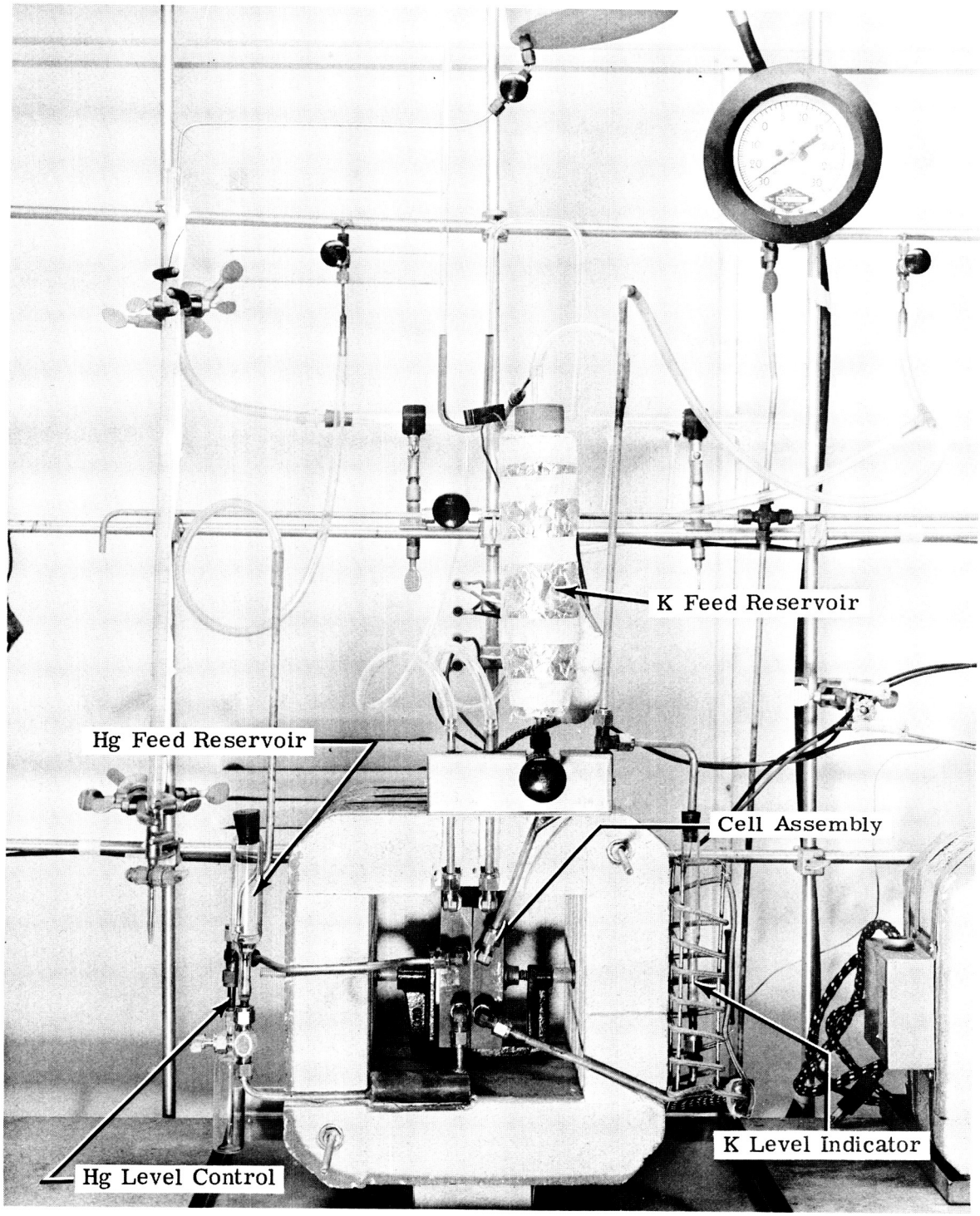

Figure 4. Small Cell Test Setup

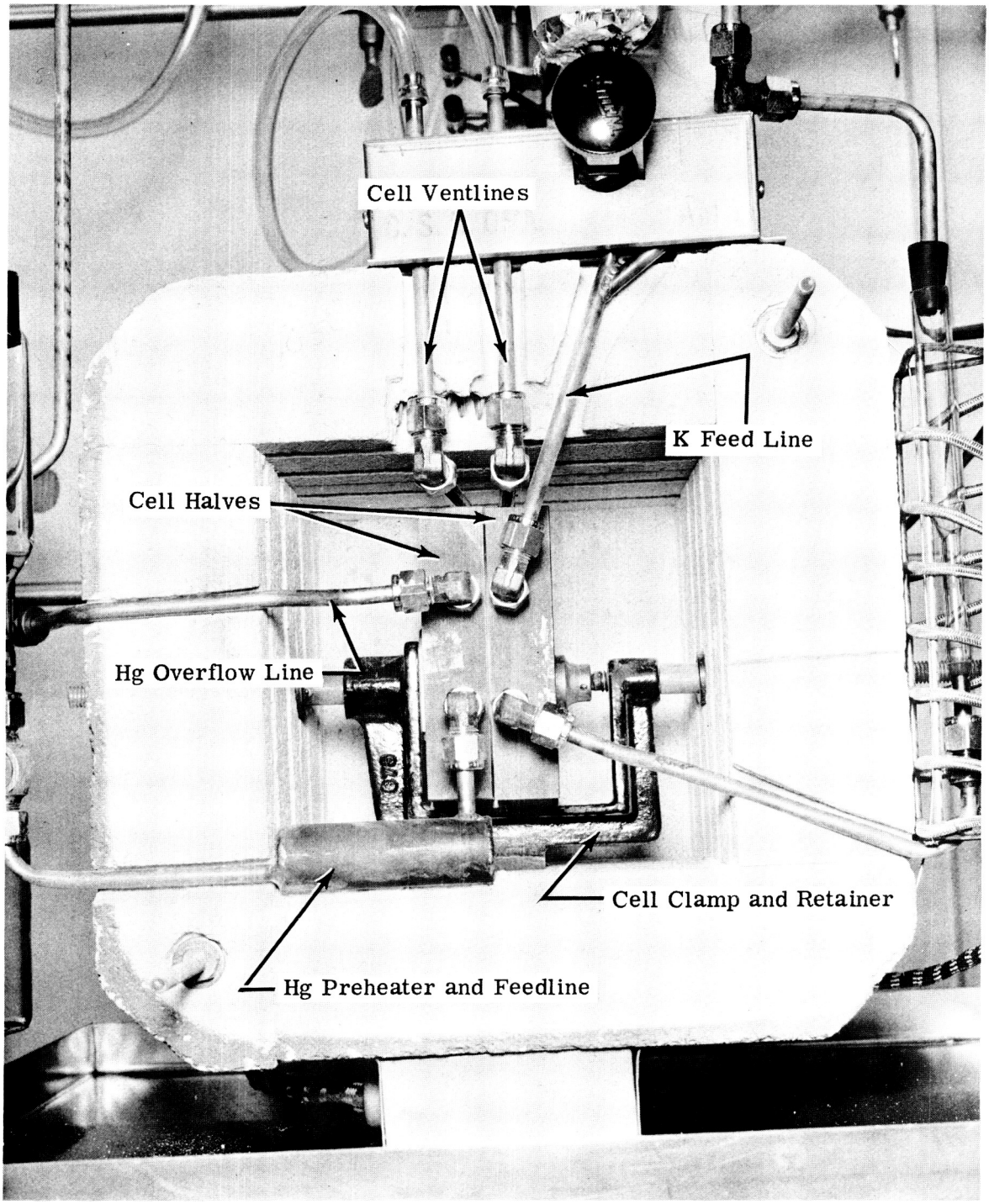

Figure 5. Small Cell Assembly

3. The Hg level is controlled by the overflow line to the lower reservoir. This reservoir will also receive the amalgam formed from electrochemical operation.

Two tests were accomplished during this reporting period. The first test was made of a coarse grain 33% electrolyte composite and gave useful electrochemical data. The second test used a fine grain 55% electrolyte composite, but had a short life due to inadequate closure of the cell to form a seal.

The electrochemical data for the first cell is shown in Table I. These data points were taken during cell operation.

TABLE I.

Data on Composite Electrolyte Matrix Cell 1

Time	Cell Potential, V_o* (volt)	Cell Voltage Under Load, V_c (volt)	Load Current, I (amp)	Computed Cell Resistance, R (ohm)	Resistivity, γ (ohm-cm)
3:20	1.05	0.63	0.67	0.627	9.91
3:30	1.02	0.66	0.59	0.610	9.64
4:05	1.00	0.43	1.00	0.570	9.01
4:16	0.75	0.26	0.725	0.680	10.75
4:35	0.88	0.28	0.78	0.770	12.17

Cell resistance is computed from an instantaneous cell potential to eliminate the effect of electrode concentration gradients. This technique is described in Figure 13 of the First Quarterly Technical Progress Report, Allison EDR 3277, and is given as

$$R_c = \frac{V_o^* - V_c}{I}$$

The primary purpose of the test was to show sealing characteristics of the composite and feasibility of the direct electrolyte-to-metal contact at the

seal region. Results of the test were positive. Some concern had been shown for the electronic conduction of the electrolyte. For this cell the effect of electronic conductance was exaggerated by the use of a contact area three times that of the active cell area. The performance shows that the electronic resistivity of the electrolyte matrix must be considerably greater than the ionic resistivity since no apparent leakage current bypassed the active cell through the seal regions.

Data on this first cell test run shows that the seal lasted for 3 hr. Potassium was held for a period of 46 min before mercury was introduced. The cell then operated at above 1 volt, open circuit, until an intermittent internal short caused instability in the voltage trace. This instability was not severe at first but became progressively disturbing until the cell was shut down. Near the end of the testing period, the change in the open circuit voltage approached half of the total value. Since an internal short has the same effect as an external load (except that the current cannot be measured), some insight into its nature can be determined. Half-load on a cell is accomplished by a load resistance equal to that of the cell internal resistance, by definition. Therefore, this cell was making and breaking very fine LM paths having a resistance of 1 ohm or less.

Figure 6 shows a photo of the cell after the matrix was removed. Sections in the seal region broke away in pieces from the center region during postmortem disassembly. Investigation showed that the center region had cracked in the plane of the disk and a piece removed during disassembly. This can be seen on the center section in Figure 6. A general breakdown of the material was evident. This breakdown extended into the seal region.

Pieces of the seal region are shown in Figure 7. A crack extends from the center out to the second serration mark. This is also the distance to which potassium had deposited onto the metal. This showed that the potassium did not progress in a flooding manner from one serration to the next in a radial direction, but moved through the fine cracks, spilling into the serration grooves and spreading around the circumference. These photos also show that the full 0.015-in. bite of the serrations into the composite was not accomplished. Apparently, the rubber seal took the clamping force

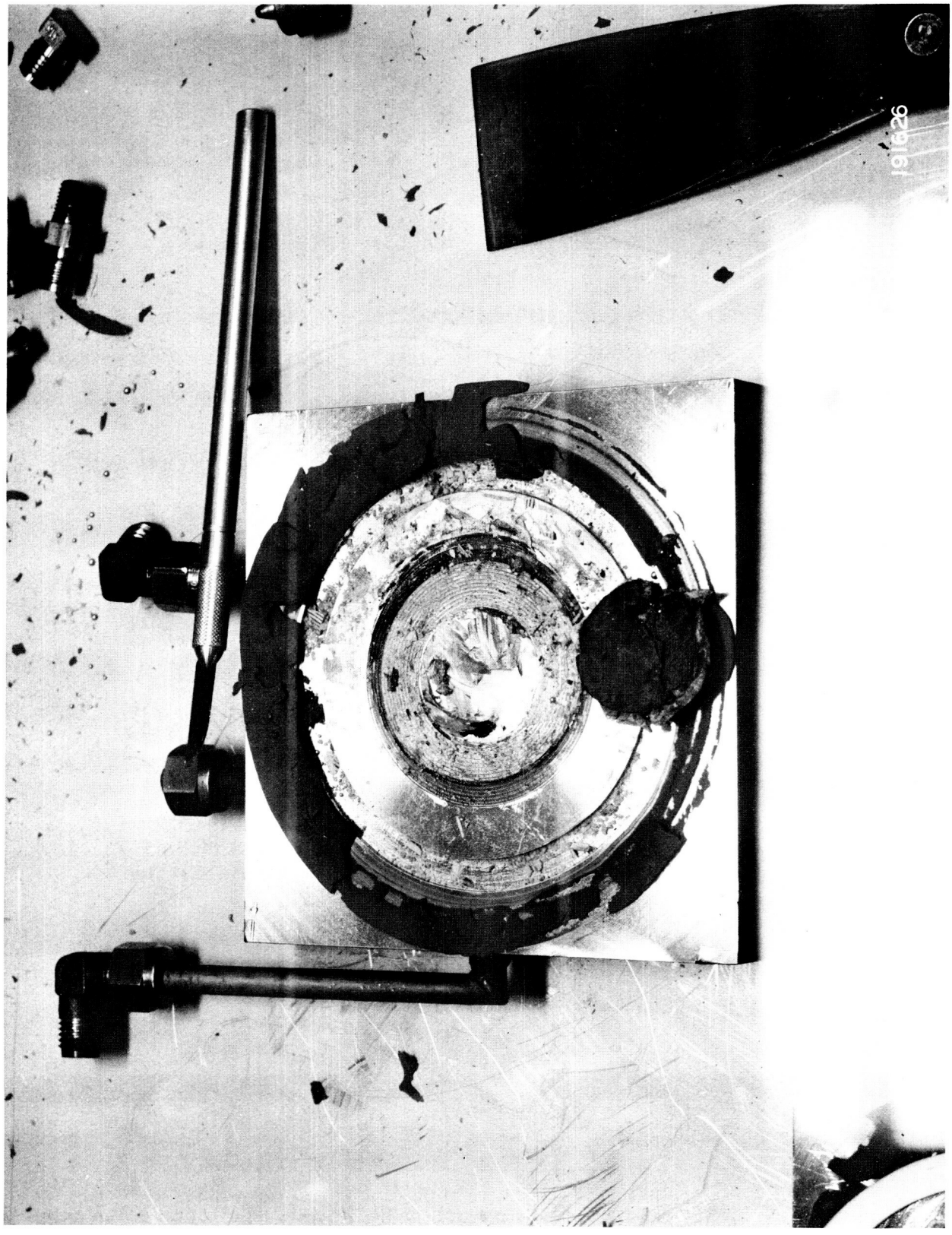

Figure 6. Cell After Matrix Removal

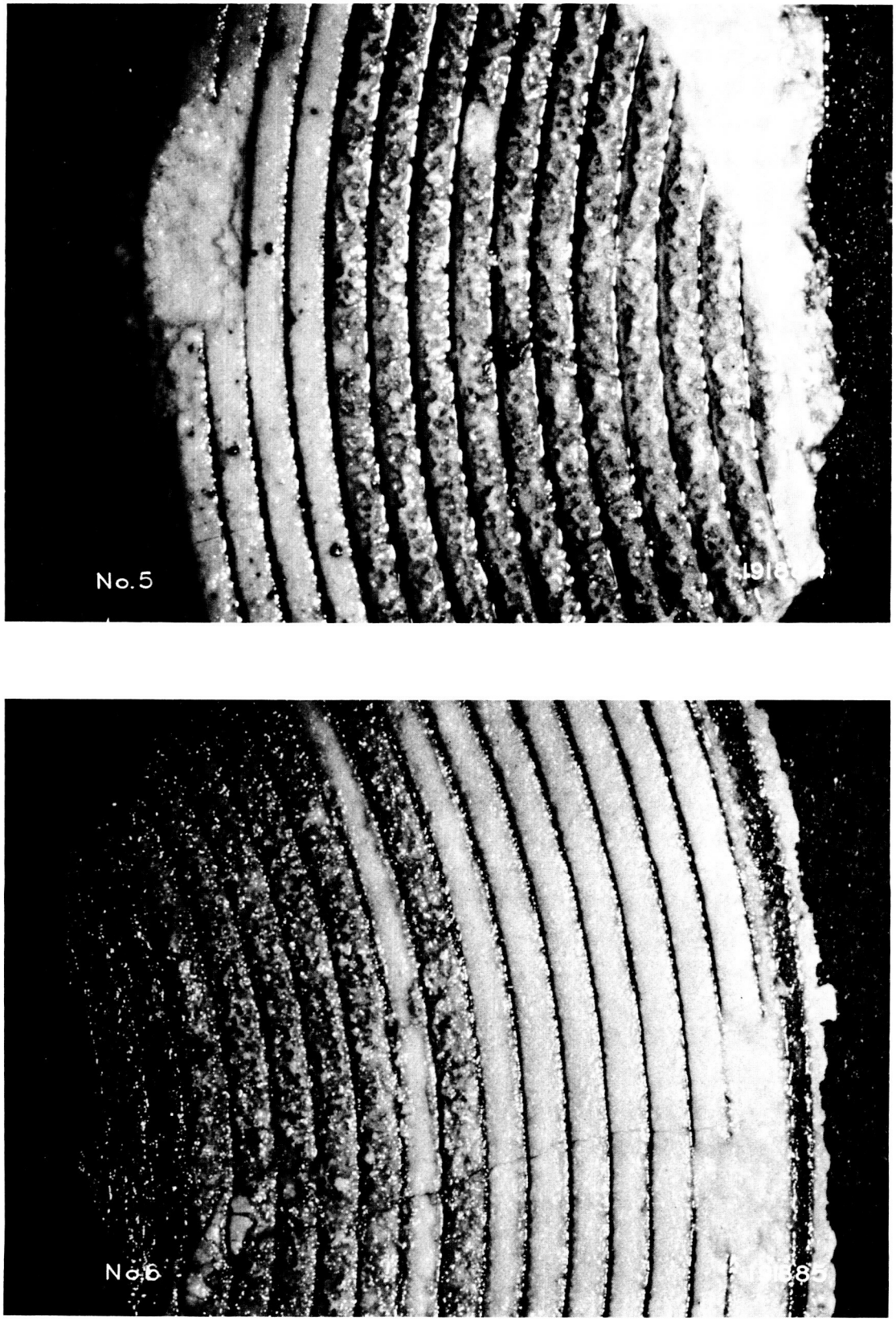

Figure 7. Sections of Matrix from the Seal Region

and acted as the stop rather than the ceramic ring. It is proposed that special silicone rubber O-rings be fabricated for later designs.

Posttest analysis of the second cell shows that the cell was not completely closed. Figure 8 shows the general flooding of the seal region by LM. Figure 9 shows the condition of the composite as it is removed from the cell, i.e., the breakup mentioned earlier. The extra heavy silicone rubber used in this cell apparently kept it from closing on one side. Lack of a seal by the concentric serrations is evident in Figure 10 when compared to those in Figure 7. This material was a newly fabricated 55% electrolyte composite which had not been tested for strength or flowability. Later work showed that this material is quite hard at cell operating temperature and, therefore, may not be ideal for a seal.

Small cell work was delayed to investigate the compatibility of the composites with the various materials and conditions to be experienced in actual cell operation.

QUALITY CONTROL STUDIES

Quality control studies were initiated to eliminate cracking of the composite. The quality control techniques used during this period are compatibility tests, radiographic inspection, and stereomicroscopic photography.

Compatibility tests were initiated and as a result it was found that the cell environment was not causing composite matrix failure. Thus, the basic concept of the unconsolidated matrix is sound. The tests were conducted in a large pyrex test tube, positioned in a furnace, and instrumented as shown in Figure 11. The composite is held by a wire harness and submerged in the liquid. The liquid is not shown, but the K metal loader is shown on top with heaters in place. A thermocouple is used to measure the liquid temperature.

The first compatibility test was run using 1-in. x 1/8-in. specimens of 33 and 35% electrolyte composite. For this test a 33% electrolyte composite specimen was submerged in mercury. The specimen was held below the surface for 24 hr at 300°C. Gassing from the specimen was observed early in the test run. Postrun analysis showed that no penetration of metal into

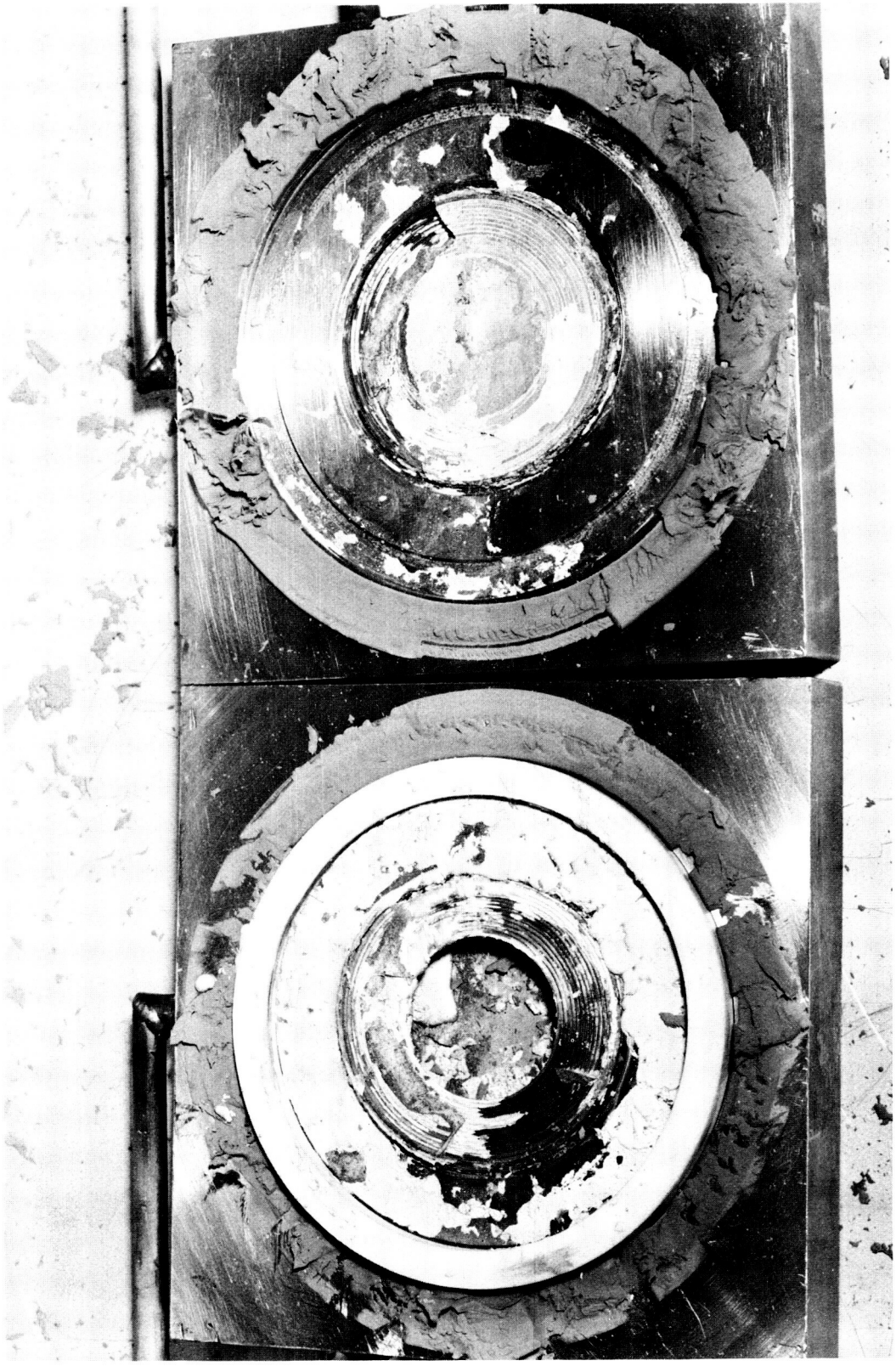

Figure 8. Second Cell Opened with Matrix in Place

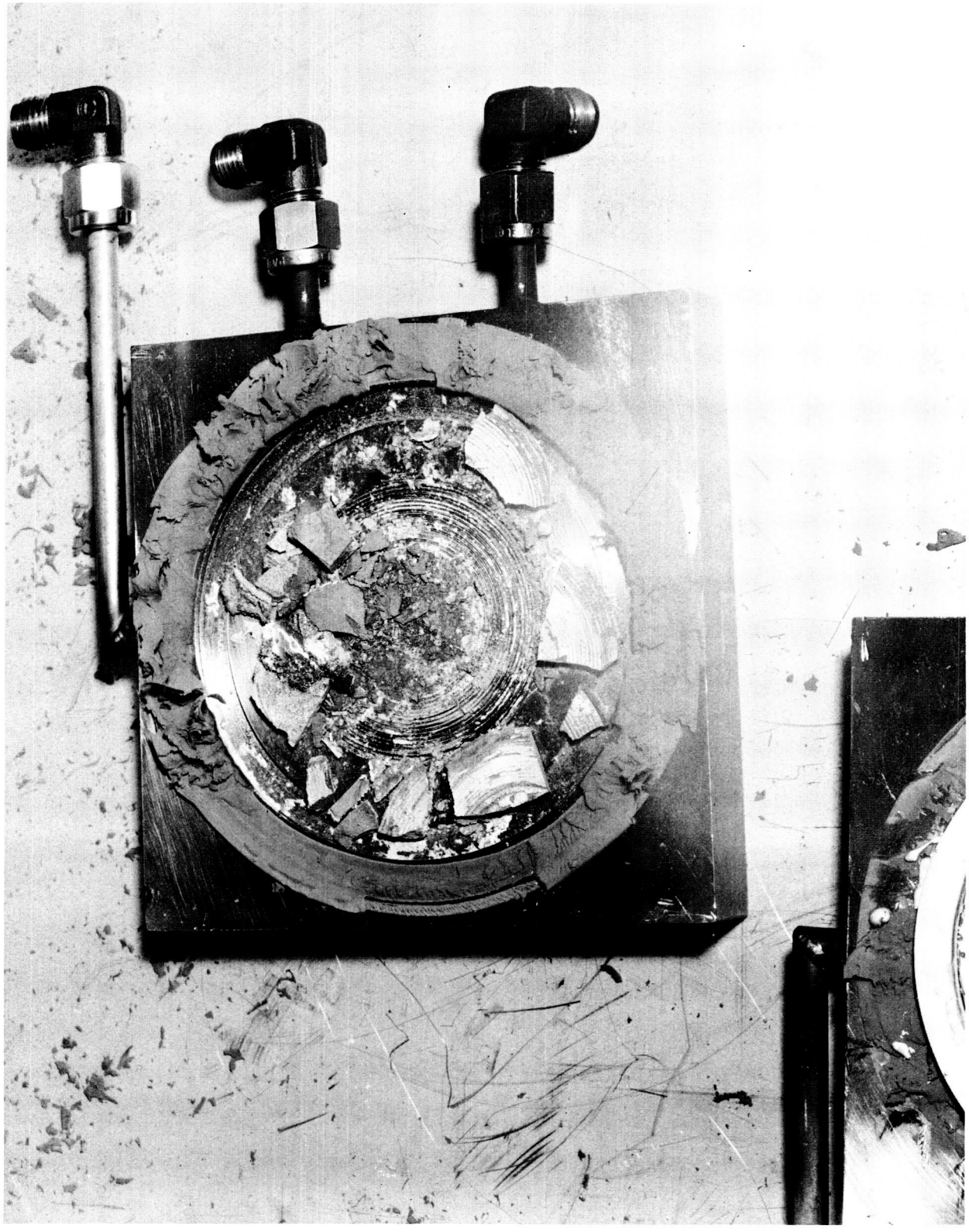

Figure 9. Matrix Removal from Second Small Cell

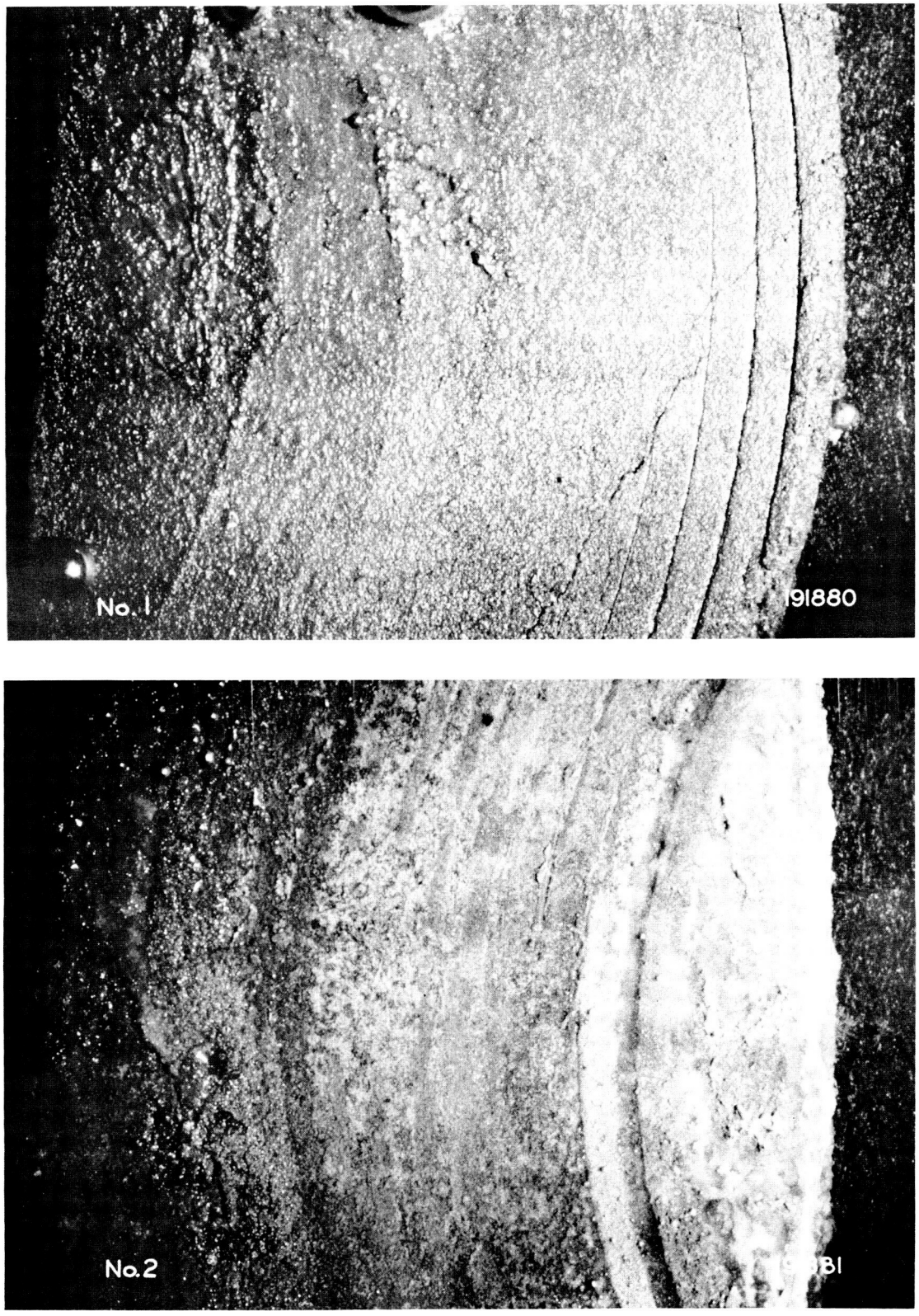

Figure 10. Sections of Matrix from Second Cell Seal Region

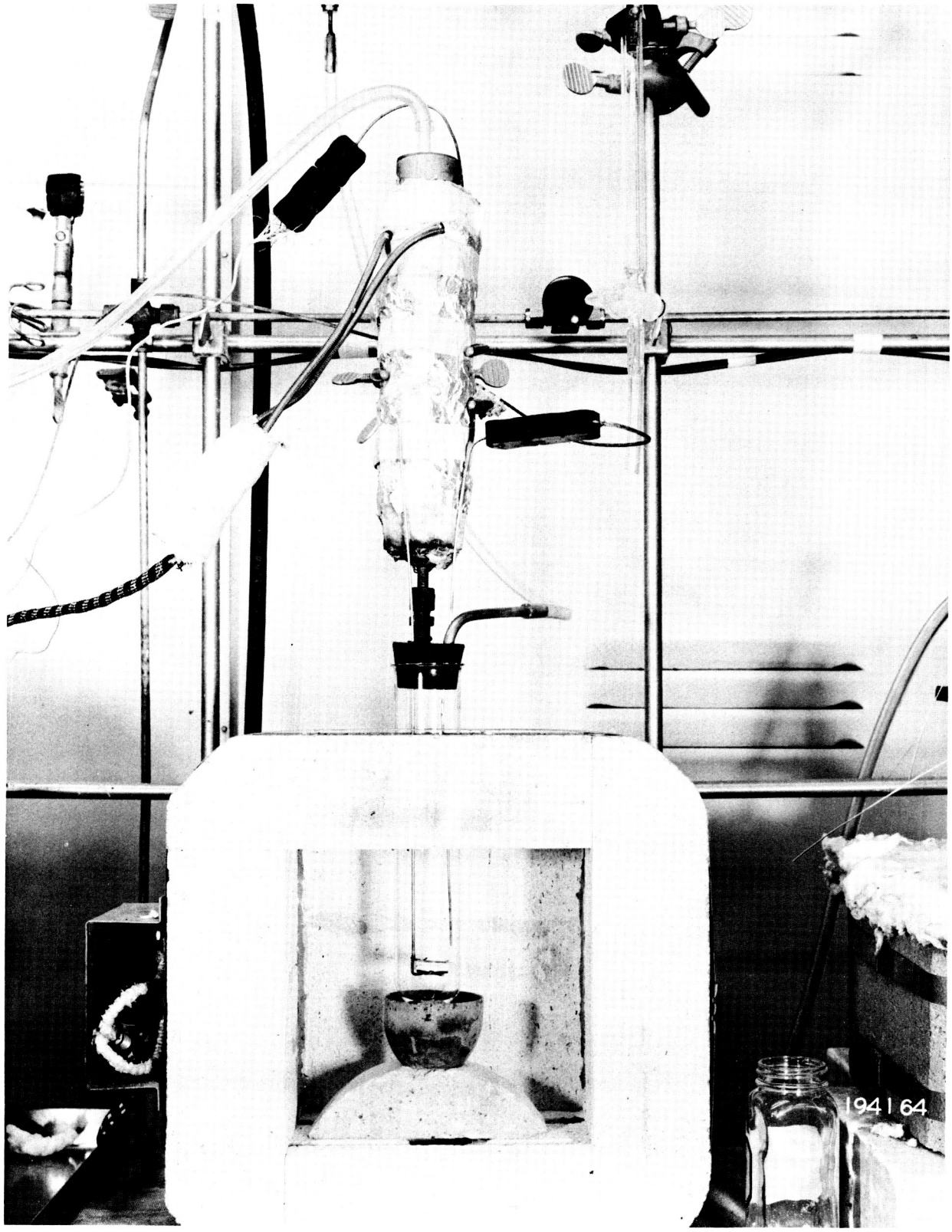

Figure 11. Test Rig for Compatibility Studies

the composite occurred. The composite also showed good strength characteristics—no deformation was observed. It is concluded that hot mercury, alone, will not destroy a composite.

The second compatibility test was performed to check the gassing observed from the composite. This was done by breaking a 33% electrolyte composite as-received under mineral oil. Microscopic examination showed that this specimen contained gas pockets. Gas was observed coming from various pockets and cracks as it was displaced by the mineral oil. Therefore, new effort will be required in the preparation of the composite to eliminate cracks, large voids, and, in general, the nonhomogeneous mixture.

A third test was carried out to check the compatibility of the composite in pure potassium. This was done with 30 gm of K metal at 300°C using 33% composite. This test only served to verify previous experiments—the electrolyte is slightly soluble in the potassium metal. As a result of 24 hr operation, all the salt dissolved into the K metal and the MgO particles settled to the bottom. Another test of this type, using a 50-50% molar K-Hg amalgam and a 35% electrolyte composite, was run for 42 min. This test was discontinued when the specimen disintegrated.

A test, incorporating a 35% electrolyte composite immersed in an electrolyte-saturated K metal, was terminated prior to immersion in the LM pool—the composite lost strength and fell from the wire harness. It was concluded that the 35% electrolyte composite, which has shown as high as 50% deformation under flowability test (as stated in the First Quarterly Technical Progress Report) does not have sufficient strength for this work without other support.

For the sixth test a newly prepared 33% electrolyte composite 1-in. x 1/8-in. was prepared. Care was taken to exclude air from the composition. This specimen was carefully preheated in the region above the electrolyte and saturated with K metal prior to immersion. A 24-hr test at 300°C was performed. The results are shown in Figures 12 and 13. Probing of the surface to remove K metal while under mineral oil revealed a large fissure

Figure 12. Electrolyte Matrix after Test Number 6—Note Cracks

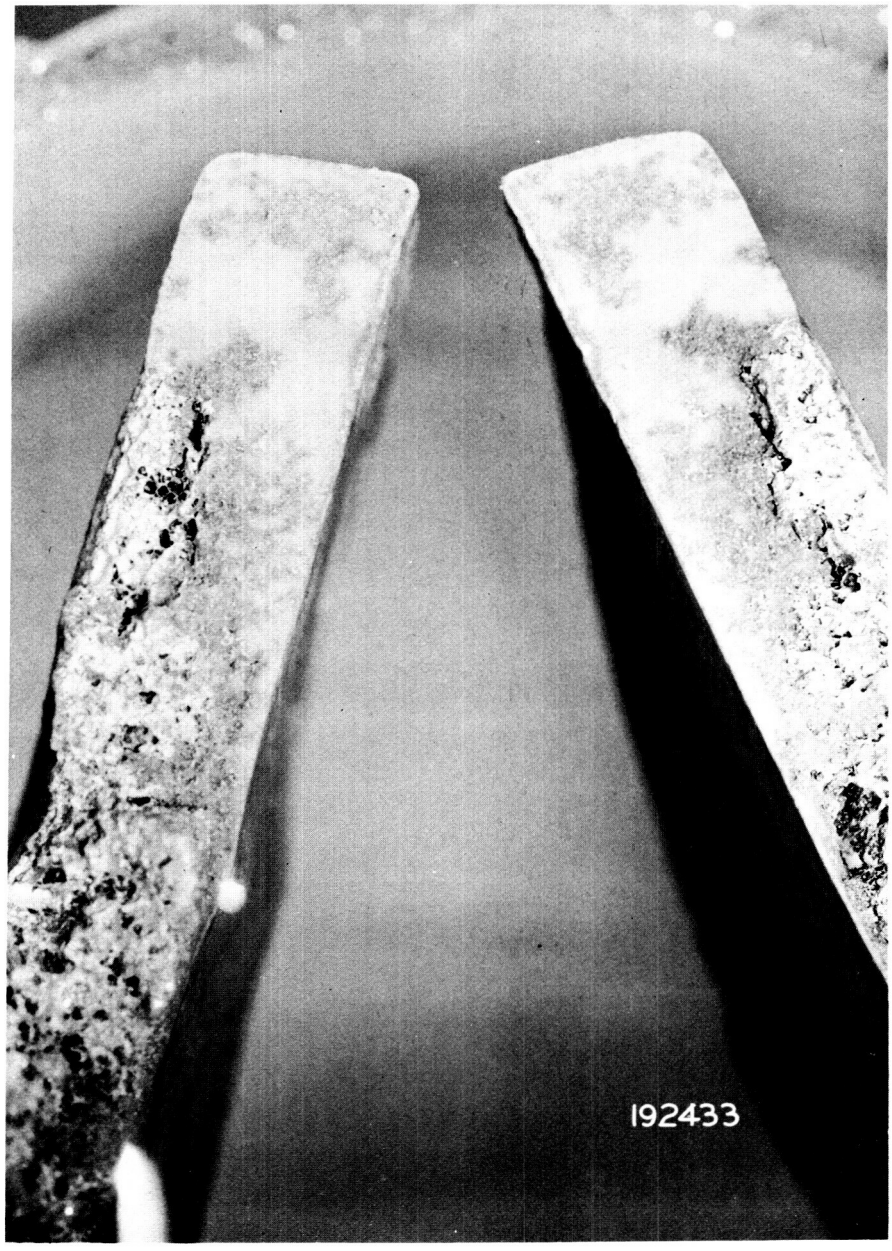

Figure 13. Broken Edges of Sixth Test Matrix — About 10% Bonded Through Cracked Area

of approximately 0.8-in. Some smaller grooves are also visible in Figure 12 which shows the specimen after it was deliberately broken along the large crack. Figure 13 shows the edge view. Only about 10% of the material was serving as a strong bond between the two halves. Potassium completely penetrated the cracked surface. The grey regions are deposits of K metal which arrived through the normal solubility of the LM into the salts.

A certain nonuniformity of structure is apparent in the "good" region. Two other specimens, which had been made at the same time, were subjected to X-ray examinations. The pictures did not reveal cracks, but it was decided that a greater effort in the development of radiography techniques would be required to interpret results. These techniques are now used for all specimens.

A seventh test was performed during this period. A 1-in. x 1/8-in. specimen was fabricated from the newly prepared 34% electrolyte composite. Since this material had been under considerable development and refinements had been made in the technique, it was anticipated to have different properties than the older batches of composites. Compatibility tests were performed after an X-ray check indicated no cracks were present. The results of this test are encouraging. This specimen was tested in an electrolyte-saturated K metal pool at 300°C for a period of 18 hr. From an outward appearance, no attack on the specimen had occurred. Figure 14 is a micrograph of a broken cross section using a stereo-zoom scope with a polaroid camera attachment. The lower photo shows that the material has many holes. The upper photo is at a higher power to study the two interconnected dark spots near the center.

The stereo-zoom polaroid micrograph technique has also been developed to include the use of stereo prints from which a 3-D effect will help interpret the surface of the microphotos. This now appears to be the only way in which this type of analysis can be accurately reported.

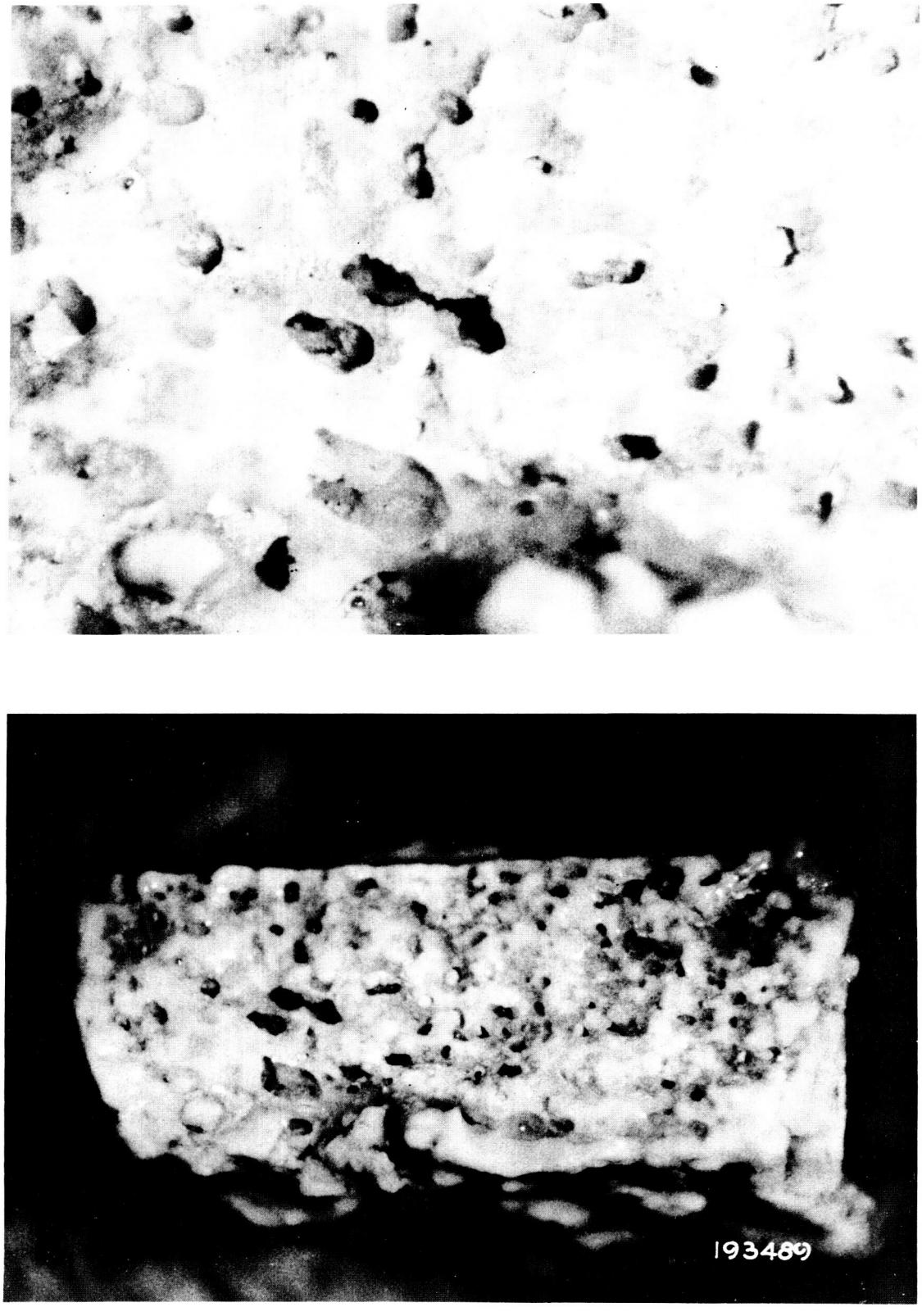

Figure 14. Micrographs of Broken Section of Seventh Test Composite Matrix

FABRICATION AND PROPERTY DETERMINATION OF COMPOSITES

The coarse grain composite work was in progress prior to this program. Early contractual effort in this area was to fill in property data not prepared in the original study by the fabrication and testing of composites. The total goal was to include electrolyte/MgO ratios from 31/69 to 35/65, and fractional theoretical densities from 72% to 89%. These data are reported and analyzed in the following paragraphs.

Fine grain composite work was proposed as a possible means for the improvement of cell performance (reference First Quarterly Technical Progress Report, Figures 8 and 9). This work has proceeded along with coarse grain investigations.

Coarse Grain Composite Work

Reporting of the coarse grain mechanical properties lagged behind the reporting of the conductivity work during the first quarter. A complete tabulation of mechanical data for the coarse grain is presented in Tables II and III.

Table II is a tabulation of the ball penetration tests performed during the first quarter. A condensed version of this table was presented in the First Quarterly Report. At that time it was thought that these data indicated a transition between the 33% and 35% composite, i.e., a change in the trend of strength variation to density for a given percent electrolyte composite. Therefore, a decision was made to work with 34/66 composite.

TABLE II.

Ball Penetration Test Results—Coarse Grain Composites

Nominal Ratio	Specimen Size* (In.)	Percent of Theoretical Density	Strength[1] (psi)
35/65	1 x 1/2	71.8	6.2
35/65	1 x 1/2	73.7	6.5
35/65	1 x 1/2	76.0	5.8
35/65	1 x 1/2	86.5	1.0
35/65	1 x 1/2	87.5	1.0
35/65	1 x 1/2	88.5	0.97
35/65	1 x 1/2	74.7	5.6
35/65	1 x 1/2	87.2	1.5
35/65	1 x 1/2	87.5	1.4
35/65	1 x 1/2	88.1	1.3
35/65	1 x 1/8	83.7	1.1[2]
35/65	1 x 1/8	83.7	1.3[2]
35/65	1 x 1/8	85.6	1.2[2]
33/67	1 x 1/2	75.3	10.1
33/67	1 x 1/2	75.3	12.3
33/67	1 x 1/2	75.6	10.1
33/67	1 x 1/2	84.6	20.2
33/67	1 x 1/2	84.9	18.5
33/67	1 x 1/2	85.9	20.2
33/67	1 x 1/8	82.1	11.1
33/67	1 x 1/8	85.3	15.8
33/67	1 x 1/8	89.7	12.3
33/67	1 x 1/8	84.3	9.2[2]
33/67	1 x 1/8	86.2	11.0[2]
33/67	1 x 1/8	86.2	7.9[2]
33/67	1 x 1/8	84.3	11.0[2]
33/67	1 x 1/8	88.8	11.0[2]

TABLE II.(cont)

Nominal Ratio	Specimen Size* (In.)	Theoretical Percent of Density	Strength[1] (psi)
33/67	1 x 1/8	90.1	10.0[2]
31/69	1 x 1/2	84.9	22.2
31/69	1 x 1/2	85.9	22.2
31/69	1 x 1/2	86.9	22.2

(1) Strength = $\frac{\text{Load}}{\text{Impression Area}}$; Load = 0.111 lb; Ball dia = 0.499 in.

(2) Load = 0.055 lb

*Specimen Size = diameter x thickness

TABLE III.

Flowability Test Results—Coarse Grain Composites

Nominal Ratio	Percent of Theoretical Density	Percent Deformation
35/65	73.7	>20
35/65	73.7	>20
35/65	74.4	>20
35/65	72.4	>30
35/65	74.7	>30
35/65	74.0	>30
35/65	73.4	40
35/65	73.4	40
35/65	74.4	50
35/65	88.5	50
33/67	75.6	40
33/67	75.6	30
33/67	74.7	> 20
33/67	85.3	30
31/69	85.9	30
31/69	86.2	20

The strength data were plotted, Figure 15, for a possible correlation as a function of the percent theoretical density and electrolyte/MgO ratio. The scatter of 33/67 data is indicated by the shaded region. These results show that there is some other variable affecting the data. If the 1/8-in. thick specimen data are discounted, the 33/67 data appear to have good correlation (dashed line). This function compared to the 35/65 data further indicates that a transition composite exists. Theoretical considerations indicate that the function displayed by the 35/65 composite should be correct for all ratios. Also, no strong argument is found for the variation in the 1/8-in. data across the transition region. Further effort to build up the understanding of this data was accomplished using a 34/66 composite during the second quarter.

The work with the 34/66 composite proved to be instructive in the area of preparation technique. Three batches of the 34/66 composite were prepared. The first batch was fabricated into conductivity, strength, and flowability test specimens and tests performed. The results of the conductivity tests on the first batch was reported in the First Quarterly Report, Figures 20, 21, and 22. The ball penetration strength data is shown in Table IV, items 1, 2, and 3. Flowability test results showed a 5% deformation at the time of edge fracture. These data do not agree with previous data obtained from flowability tests which show 33/67 composites as 30% deformation and 35/65 composites as 40% or greater deformation. Therefore, the composite was deemed questionable and a new batch was prepared for verification of results.

Difficulty was encountered in preparing the second batch—therefore a third batch was prepared. Conductivity work with the third batch is in process. The ball penetration strength test results are tabulated in items 4-11 in Table IV. New flowability results are given in Table V, and are discussed in a later section.

All 34/66 ball penetration strength data from Table IV are plotted in Figure 16. The analysis of these results is as follows.

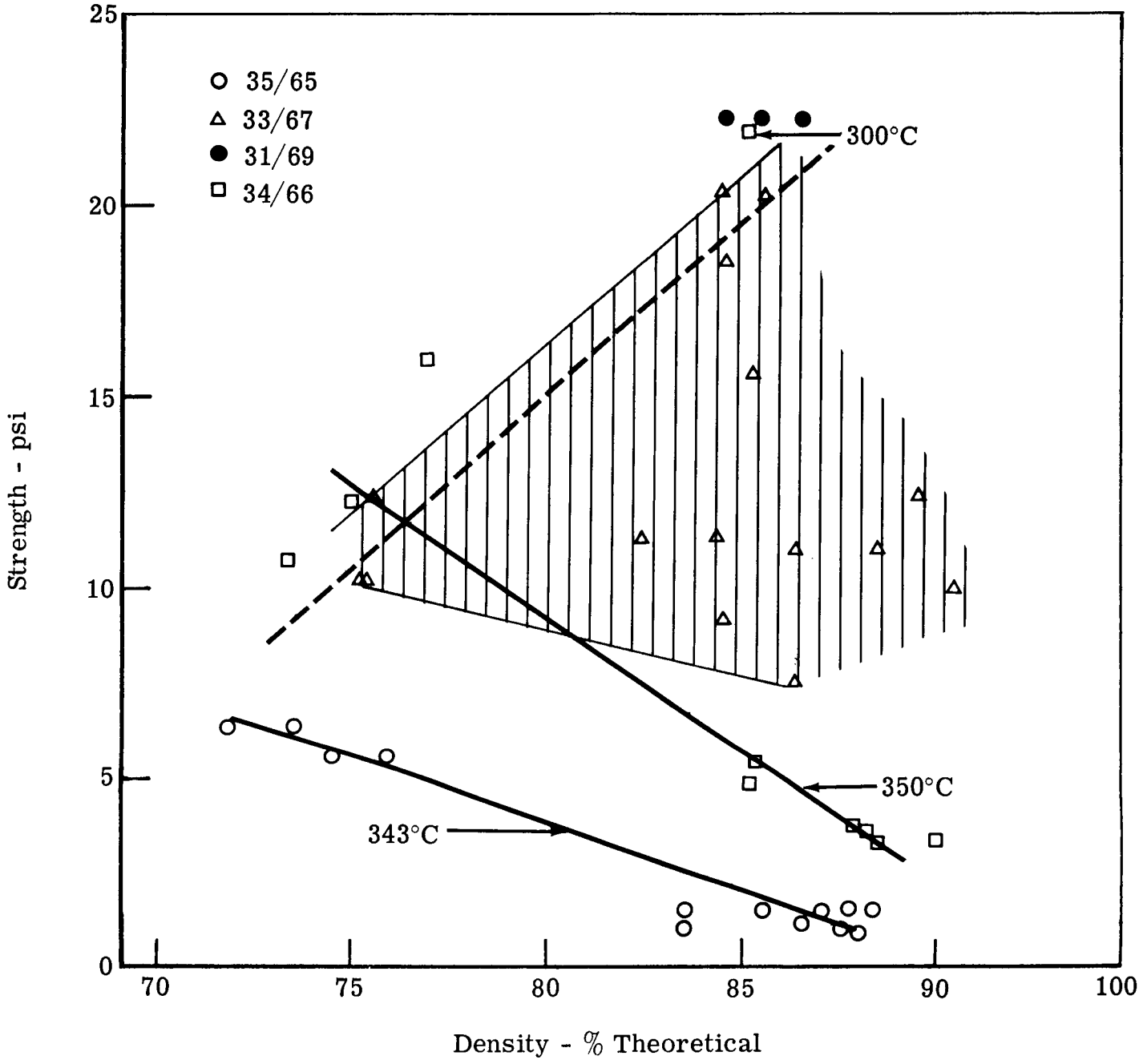

Figure 15. Ball Penetration Strength Test Results

TABLE IV.

Ball Penetration Test Data—34/66 Coarse Grain Composite

	Percent of Theoretical Density	Strength (psi)	Temperature (°C)
1.	85	5	350
2.	85	6.5	350
3.	90	3.6	350
4.	74.7	12.3	350
5.	77.2	15.9	350
6.	73.1	11.1	350
7.	87.5	3.4	350
8.	86.2	3.4	350
9.	88.1	3.3	350
10.	85.3	22	300
11.	85.3	22	300

1. Results from the first and third batches agree, and it is further believed that these batches agree with respect to both conductivity and strength. The poor flowability results, then, may have been caused by an unknown variable in the preparation technique which affects surface strength.

2. The 34/66 lower density data has a fair correlation with previously obtained low density data from 33/67 composite for the 350°C tests. Therefore, the linear function shown for this data now shows correlation with 35/65 data. This also follows the theory that predicts a decrease in strength with an increase in saturation caused by either an increase in the electrolyte/MgO ratio or a higher percent of theoretical density.

3. The results from the 300°C tests are much higher than those for the 350°C tests; therefore, showing a predicted trend for the composite to become weaker with an increase in temperature.

4. Since there is good correlation of 350°C low density data it is not plausible that the dashed line describes the strength function of a 33/67 composite. It is more likely that the data in the region around the 34/66 composite data run at 300°C is of a group of specimens which were run cooler than anticipated. Therefore, it would follow that the other 33/67 data is a scatter caused from temperature variation.

   Further work with the coarse grain composite will be required to completely resolve this strength variation.

Flowability data for the coarse grain work are shown in Table III. A summary of these data was given in the First Quarterly Report, Table V. The complete list shows the exact value for density, but an indefinite or rounded-off value for deformation. The first six values show that fracture did not occur up to that percent deformation and therefore must be greater than the value given.

Later work with 34/66 composite gave the results shown in Table V.

As a trend, flowability increases with an increase in saturation. This trend appears to be independent of temperature, at least in the range tested.

A later testing technique gave better measurement of the deformation, but the largest possible error in this work appears to be in the detection of fracture. Therefore, it is not intended that present data constitute an absolute measure of a yield point for this material. Further, the strengths given by the ball penetration test are only good as a measure of relative values, one specimen to another. Program plans are for use of other supporting members in conjunction with the paste to gain strength so that a thin, large area matrix can be incorporated in cell design.

TABLE V.

Flowability Test Data—34/66 Coarse Grain Composite

	Percent of Theoretical Density	Deformation to Failure (%)	Temperature (°C)
1.	77	19	350
2.	75	19	350
3.	86	25	350
4.	87	28	350
5.	87	17	350
6.	90	27	300
7.	90	32	300

Fine Grain Composite Work

Work on the fine grain composite started with the present program. Earlier work had gone into the selection and procurement of the ceramic material. Attempts to fabricate a composite by use of the original wet process, used for the coarse grain, failed. A new dry process was developed, as reported in the First Quarterly Report, and made possible the fabrication of the first test specimens. Difficulty with surface blistering continued to hinder the fabrication of specimens through the second quarter on mass ratios of 55/45, 57.5/42.5, and 60/40. Considerable data have been obtained on both conductivity and strength from these specimens and is reported in the hope that further work will verify the validity.

Conductivity

The conductivity data are listed in Tables VI and VII. Table VI identifies the specimen, and Table VII identifies the temperature and conductivity data.

TABLE VI.

Conductivity Specimen Identification

Specimen No.	Nominal Weight Ratio	Percent of Theoretical Density	Diameter (in.)	Height (in.)	Test Height (in.)
36	55/45	90.9	0.598	0.687	0.603
37	55/45	88.2	0.601	0.685	—
38	55/45	90.9	0.598	0.689	0.613
39	57.5/42.5	82.7	0.610	0.708*	0.675
40	57.5/42.5	82.7	0.610	0.683	0.663
41	57.5/42.5	81.3	0.610	0.668	—
42	60/40	89.0	0.607	0.628	0.598
43	60/40	88.0	0.610	0.630	0.610
44	60/40	87.0	0.612	0.647	0.609

*Reworked before testing

TABLE VII.

Conductivity Specimen Data

Specimen No.	Temperature (°K)	Resistance (ohm)	Conductivity (mho/cm)	$\frac{1}{T} \times 10^3 (°K)^{-1}$
36	628	2.12	0.46	1.59
	595	2.70	0.36	1.68
	570	3.37	0.29	1.75
	537	4.92	0.20	1.86
37	626	2.70	0.36	1.60
	605	3.10	0.30	1.65
	577	3.86	0.25	1.73
	551	5.00	0.19	1.81
38	635	2.04	0.47	1.57
	602	2.62	0.37	1.66
	577	3.33	0.29	1.73
	541	4.80	0.20	1.85
39	625	2.62	0.36	1.60
	610	3.00	0.32	1.64
	581	3.74	0.25	1.72
	543	5.10	0.19	1.84
40	642	2.49	0.37	1.56
	611	3.07	0.30	1.64
	580	3.97	0.24	1.72
	540	5.71	0.16	1.85
41		Broken Specimen		
42	639	1.90	0.45	1.56
	616	2.25	0.38	1.62
	576	2.96	0.29	1.74
	552	3.74	0.23	1.81
43	646	1.95	0.44	1.55
	616	2.35	0.36	1.62
	592	2.75	0.31	1.69
	543	4.39	0.19	1.84
44	643	1.84	0.47	1.56
	612	2.24	0.39	1.63
	585	2.76	0.32	1.71
	547	3.89	0.22	1.83

Specimens 39 and 40 were nearly identical in properties. Since 39 had greater height, the end deposit was scraped off for chemical analysis. This deposit emanates from the material on which the specimen rests for the final bake-out in the fabrication process. The analysis showed that minor portions of Na, Mg, and Ni along with traces of Cu, Cr, and Fe were present. Subsequent conductivity runs on these two specimens enabled the effect of this deposit on the contact resistance in the conductivity apparatus to be observed. All data are plotted in Figure 16. It can be seen that the conductivity for specimen 39 runs slightly higher than that for specimen 40.

Since the fine grain composite work has not yet been optimized for strength, it can not be determined that these data represent the final fine grain performance. However, the value at cell temperature may run as high as 0. 30 mho/cm. When compared to values of 0. 10 mho/cm for the coarse grain—an improvement factor of 2 to 3 is realized.

Mechanical Strength

Ball penetration and flowability data for the four fine grain composites are given in Tables VIII and IX. Strength increases with an increase in temperature according to these readings. Since percent of theoretical density is not reported, it is difficult to glean much information from these results. A strength-temperature relation of this type is not predicted from theory, and reports that this material has displayed blistering during bake-out procedures indicate that a possible surface strength is detected by these results. The normal decrease of strength with a higher electrolyte content is shown and therefore may indicate a trend of the subsurface material to follow the predicted trends.

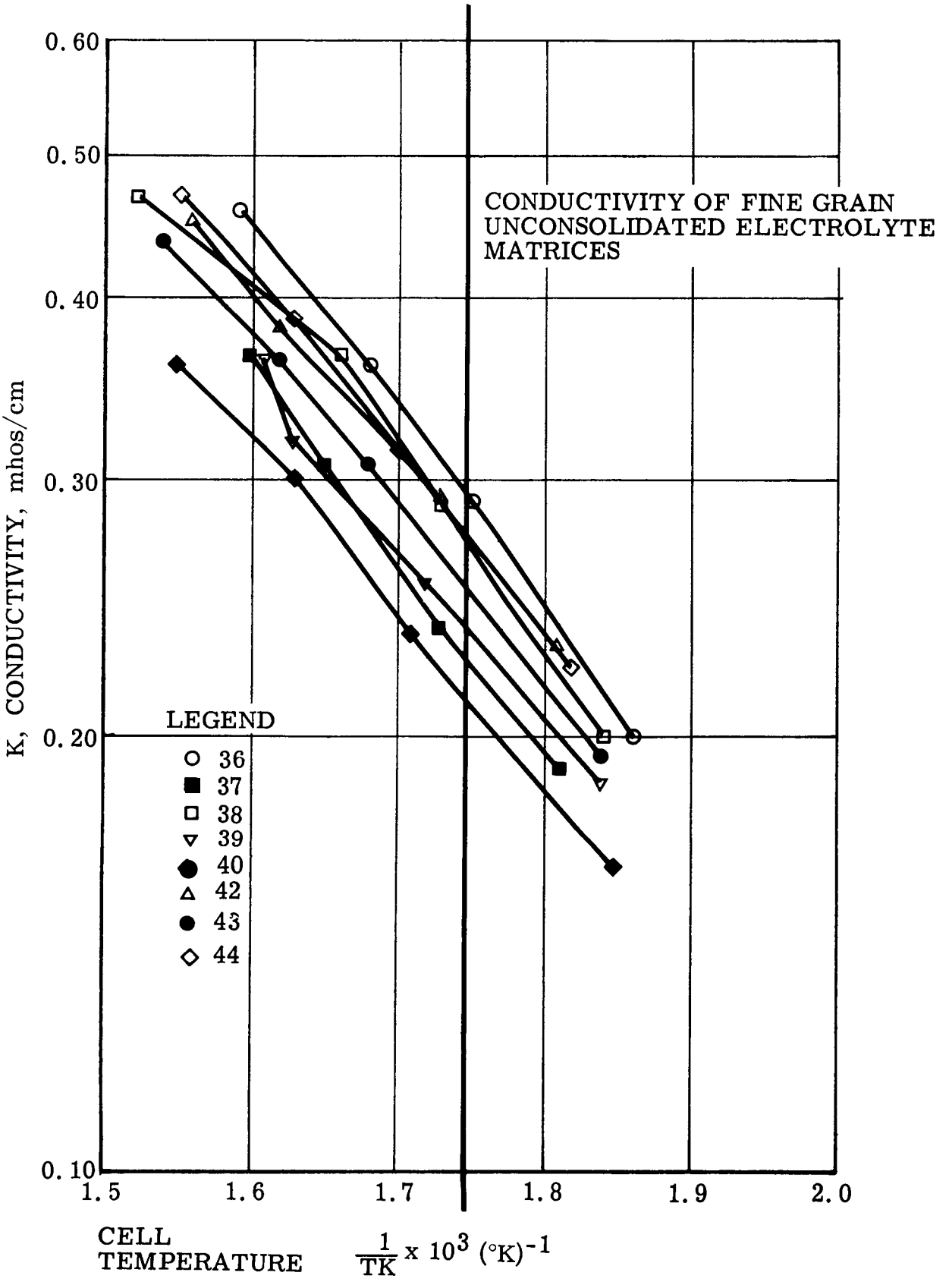

Figure 16. Conductivity of Fine Grain Unconsolidated Electrolyte Matrices

TABLE VIII.

Ball Penetration Test Results—Fine Grain Composites

Nominal Weight Ratio	Percent of Theoretical Density	Strength (psi)	Temperature (°C)
55/45		2.7	250
		2.8	250
		2.4	300
		2.5	300
		12.3	350
		10.1	350
57.5/42.5		1.9	300
		8.7	350
		8.7	350
		8.0	350
60/40		1.9	300
		1.8	300
		2.9	350
		2.9	350
		3.0	350
63/37	90%	2.5	300

TABLE IX.

Flowability Test Data—Fine Grain Composites

Nominal Weight Ratio	Percent Deformation	Temperature (°C)
55/45	16.1	250
	21.1	250
	10.4	300
	9.1	300
	4.3	350
	4.2	350
	3.6	350
57.5/42.5	12.7	300
	3.9	350
	4.0	350
60/40	12.3	300
	9.9	350
	9.0	350
	9.8	350

Flowability data show the same increase trend as mentioned previously. Since the cracking of the surface is the "detector" for the test, then surface hardening will give an early indication of the deformation limit. These data for fine grain composites show that trouble has been encountered. Observations of cracking during composite fabrication indicate that a critical review of the procedures is necessary to find a means for eliminating moisture and/or gas from the specimens. Recent work with 63/37 composite using a newly prepared electrolyte eutectic has shown some changes in the properties and may prove to be the break-through in fine grain work. This work will continue during the third quarter.